Concentration Dependence of the Interfacial Tension of Polymer Solutions near Repulsive Walls and in Good Solvent

C. Redon, D. Ausserre,† and F. Rondelez*

Laboratoire de Physico-Chimie des Surfaces et Interfaces, Institut Curie,‡ Section de Physique et Chimie, 11, rue Pierre et Marie Curie, 75231 Paris Cedex 05, France

Received March 4, 1992; Revised Manuscript Received May 19, 1992

ABSTRACT: We have performed contact angle measurements for sessile droplets of poly(styrene)–toluene solutions deposited on low-energy solid substrates. In this system where the chains are repelled at both the solid/liquid (S/L) and at the liquid/vapor (L/V) interfaces, we observe that the contact angle *increases* with polymer concentration. From these measurements, we derive the surface tension variations $\Delta\gamma$ over a wide range of concentrations, c (up to 3 g/g), and molecular weights, M_w (10^5–3×10^6), covering both the dilute and semidilute regimes. At low concentration (dilute regime), the surface tension increases proportionally with c. At larger concentrations (semidilute regime), $\Delta\gamma$ increases as $c^{3/2}$ and becomes molecular weight independent. These results allow a simple, yet clear-cut, test of the scaling law predictions for the behavior of polymer chains near repulsive interfaces, in good solvent conditions.

Introduction

Mean-field[1–3] and scaling theories[4–6] have been developed by several authors to predict the interfacial properties of polymer solutions. They distinguish two basic situations: (i) the polymer chains are adsorbed at the interface and the local polymer-chain concentration is therefore higher near the wall than in the bulk and (ii) the polymer chains are pulled away from the wall by entropic repulsion forces and this creates depletion layers at the interface. Experimental studies of the polymer concentration profiles at the solid/liquid and liquid/vapor interfaces have been performed by using optical and X-ray evanescent wave techniques[7,8] and more recently by neutron reflectivity and neutron scattering.[9–11] These methods require special sophisticated setups, however, which are not available to all laboratories. We present here simple contact angle measurements of a sessile droplet of polymer solution deposited on solid substrates which immediately reveal if the polymer chains in the solution are repelled or attracted by the interfaces. The experiments have been performed in good solvent conditions, over a large range of polymer concentration covering both the dilute and the semidilute regimes, and for molecular weights between 10^5 and 3×10^6. The poly(styrene)–toluene system which has been investigated corresponds to repulsive conditions, and we show that in this case both the liquid/vapor and the liquid/solid interfacial tensions can be derived from contact angle data.

First, we give a brief summary of the existing theories and emphasize the main assumptions of our model. We then describe the experimental setup and present the contact angle measurements as a function of polymer concentration and molecular weight. The experimental results for the surface tension variations, $\Delta\gamma$, are discussed in the framework of the scaling law theory. Finally, we compare our findings to an earlier determination of $\Delta\gamma$ at the liquid/vapor interface and we discuss the applicability of the method to other polymer–solvent systems.

Theoretical Background

When a sessile droplet is deposited on a solid substrate, the equilibrium contact angle θ is related to the surface tension γ_{lv}, γ_{ls}, and γ_{sv} at the liquid/vapor, liquid/solid, and solid/vapor interfaces, respectively, through the classical Young relationship:

$$\gamma_{lv} \cos\theta = \gamma_{sv} - \gamma_{ls} \tag{1}$$

In the case where the liquid is a polymer solution, the two quantities γ_{lv} and γ_{ls} are expected to depend on the polymer volume fraction ϕ. On the contrary, the solid/vapor surface tension γ_{sv} is assumed to be independent of the polymer concentration since the vapor pressure of the polymer in the gaseous phase is close to zero. We neglect here the fact that the chemical potential of the solvent in the vapor phase is a function of the polymer concentration in the drop. Such effects, which would induce variations of γ_{sv} with ϕ, are certainly negligible in our low polymer concentration range ($\phi < 0.3$). Indeed, an approximate calculation gives a $\Delta\mu/RT$ change of 3×10^{-3} for $\phi = 0.15$, when the value $\chi = 0.44$ found in the handbook tables for the poly(styrene)–toluene system is used.[12]

The Young equation (1) can be rewritten to emphasize the functional dependence of γ_{sl} and γ_{lv} on ϕ:

$$\gamma_{lv}(\phi) \cos\theta(\phi) = \gamma_{sv} - \gamma_{ls}(\phi) \tag{2}$$

For the pure solvent ($\phi = 0$), one has

$$\gamma_{lv}(0) \cos\theta(0) = \gamma_{sv} - \gamma_{ls}(0) \tag{3}$$

Subtracting (3) from (2) allows the elimination of γ_{sv}, and one then obtains

$$(\gamma_{lv}(0) + \Delta\gamma_{lv}) \cos\theta - \gamma_{lv}(0) \cos\theta_0 = -\Delta\gamma_{ls} \tag{4}$$

where we have set $\theta_0 = \theta(0)$ and $\Delta\gamma = \gamma(\phi) - \gamma(0)$.

This equation shows that $\Delta\gamma_{ls}$ and $\Delta\gamma_{lv}$, which represent the variation of the solid/liquid and liquid/vapor surface tensions, respectively, with the polymer volume fraction ϕ, are directly related to the equilibrium contact angel θ.

In the particular case where the interactions between the polymer chains and the two interfaces are governed by purely repulsive entropic forces, one can assume

$$\Delta\gamma_{ls} \approx \Delta\gamma_{lv} \equiv \Delta\gamma \tag{5}$$

This will be justified below in the Discussion. Equation

* To whom correspondence should be addressed.
† Present address: Université du Maine 72017 Le Mans, France.
‡ Laboratoire associé au CNRS (URA No. 1379) et à l'Université Pierre et Marie Curie.

0024-9297/92/2225-5965$03.00/0

4 then becomes

$$\frac{\Delta\gamma}{\gamma_{lv}(0)} \approx \frac{\cos\theta_0 - \cos\theta}{1 + \cos\theta} \tag{6}$$

Calculation of the Surface Tension Variations $\Delta\gamma_{ls}$ and $\Delta\gamma_{lv}$. There are two regimes of chain behavior depending on the average distance between polymer coils.[5]

(1) When the average distances between the chains is larger than the radius of gyration for a single chain, R_g, the solution can be considered as a dilute solution of individual coils of radius R_g. When this solution is in contact with a repulsive wall, the excluded volume effect will restrict the chains to approach the wall at a distance smaller than R_g. The corresponding surface tension increase can be estimated by considering the work required to create the depletion layer of length R_g against the osmotic pressure, Π_d,[5] where the subscript "d" indicates dilute regime. For a dilute solution, Π_d is proportional to the number of polymer chains per unit volume, i.e. $\Pi_d \sim (c/M)RT$, where M is the molecular weight, c the concentration in g/cm^3, T the temperature, and R the gas constant. This leads to the simple equation

$$\gamma - \gamma_0 \sim \Pi_d R_g \sim cN^{\nu-1} \sim cN^{-0.4} \tag{7}$$

where N is the number of monomers per chain and ν the Flory exponent. For flexible chains in good solvent conditions, $\nu = {}^3/_5$.

In the dilute regime, the difference between the surface tension of the pure solvent, γ_0, and that of the polymer solution, γ, is thus a linear function of the polymer concentration and depends on polymer molecular weight as $N^{-0.4}$.

The weight fraction c is related to the polymer volume fraction ϕ by

$$\phi = \frac{c}{c + (1-c)\dfrac{d_s}{d_p}} \tag{8}$$

where d_p and d_s are the polymer and solvent densities, respectively. At low concentration, $c \ll 1$ and $\phi \approx (d_p/d_s)c$.

(2) When the average distance between the chains is smaller than R_g, the polymer chains overlap and form a transient network of characteristic length, ξ, which depends on polymer volume fraction as $\xi \sim \phi^{-3/4}$ in the good-solvent case.[5] This semidilute regime, indicated in the following by the subscript "sd", is only defined for ϕ higher than $\phi^* \approx NR_g^{-3}$, the overlap fraction. Near a wall, the thickness of the depletion layer is ξ and the surface tension increment is now due to the work against the osmotic pressure, Π_{sd}, and over the distance ξ. The prediction for the ϕ dependence of Π_{sd} is $\Pi_{sd} \sim RT/\xi^3$, which expresses the fact that a semidilute solution can be viewed as an ideal solution of "blobs", of average size ξ. Therefore, this leads to the equation

$$\gamma - \gamma_o \sim \Pi_{sd}\xi \sim \frac{RT}{\xi^3}\xi \sim \phi^{3/2} \tag{9}$$

In the semidilute regime, the difference between the surface tension of the pure solvent, γ_0, and that of the polymer solution, γ, is thus a scaling function of the polymer volume fraction with an exponent ${}^3/_2$. Moreover, a characteristic of the semidilute regime is that $\gamma - \gamma_o$ is now independent of molecular weight.

Simplified Calculation of the Contact Angle Variations $\theta_0 - \theta$ in the Dilute Regime. In the dilute regime, one can simplify eq 6 by expanding cos θ around cos θ_o because, for small concentration values, the contact angle variations should obviously be very small. This leads to

$$\frac{\Delta\gamma}{\gamma_{lv}(0)} \approx \frac{\cos\theta_0 - \cos\theta}{1 + \cos\theta_0} \approx \tan\left(\frac{\theta_0}{2}\right)\Delta\theta + O(\epsilon^2) \tag{10}$$

where $\Delta\theta = \theta - \theta_0$ and $\epsilon = \cos\theta - \cos\theta_0$.

Combining eqs 7 and 10, one readily observes that, in the dilute regime, the contact angle varies linearly with the polymer concentration:

$$\Delta\theta \sim c \tag{11}$$

By contrast, in the semidilute regime, the approximation $\cos\theta \approx \cos\theta_0$ is no longer valid and we have to use the full eq 6 to calculate the variation $\Delta\gamma$ and study its dependence on polymer volume fraction, ϕ.

Experimental Section

(1) **Contact Angle Measurements.** The setup used to measure the contact angles has already been described in ref 13. The drop is deposited on a transparent substrate and illuminated from above by using a low-power He–Ne laser. The collimated light beam is deflected by the edge of the liquid drop which locally acts as a prism. If the beam size is larger than the drop diameter d, the drop behaves on the whole as a planoconvex lens. A converging cone of light thus emerges from the sample, and its apex angle θ'' is calculated by measuring the beam diameter, D, onto a screen located at a known distance h from the drop. One has

$$\tan\theta'' = \frac{D + d}{2h} \tag{12}$$

where d is the drop diameter obtained independently by measuring the dimension of the drop shadow on the screen.

The contact angle θ is easily deduced from θ'', by using geometrical optics:

$$\tan\theta = \frac{-\sin\theta''}{1 - (n(\phi)^2 - \sin^2\theta'')^{1/2}} \tag{13}$$

To calculate θ, it is however necessary to know the refractive index variation $n(\phi)$ with the polymer volume fraction. These values can be obtained by using the relationship

$$n(\phi) = n_s + \frac{dn}{d\phi}\phi \tag{14}$$

where n_s is the solvent refractive index and $dn/d\phi$, the specific refractive index increment. For the poly(styrene)–toluene system, $n_s = 1.49$ and $dn/d\phi = 0.10$.[14] This leads at most to a 1% correction in our case where $\phi < 0.3$. We assume here that $n(\phi)$ is homogeneous throughout the liquid drop.

Figure 1a is a sketch of the experimental setup whereas Figure 1b shows an example of the observed transmission pattern through the drop. In this particular case, the drop diameter was 3 mm, from which the contact angle was calculated to be 35°. The whole apparatus was enclosed in an air-tight enclosure which was saturated with solvent vapor by putting a large reservoir of solvent next to the substrate and letting the atmosphere equilibrate for several tens of minutes. A syringe S with a long stainless steel needle was introduced through a septum, and a liquid droplet was slowly deposited until a stable advancing contact angle was achieved. Measurements were found to be highly reproducible, typically to within 0.2°. That gave a mean relative accuracy of better than 1%, for θ_a values around 40°.

Receding contact angles, θ_r, were measured by sucking a small amount of liquid back into the syringe. In the case of our repulsive surfaces, the hysteresis amplitude, $\theta_a - \theta_r$, was never larger than 4–5°. This is small compared to the typical hysteresis values obtained on untreated surfaces, which are usually well above 10°.

The above procedure can be used for the $\theta(\phi)$ measurements both on pure solvent and on dilute polymer solutions. When the volume fraction becomes too large, especially at high molecular weight, the viscosity η is such that the liquid can no longer be pushed through the narrow hypodermic needle. In such cases,

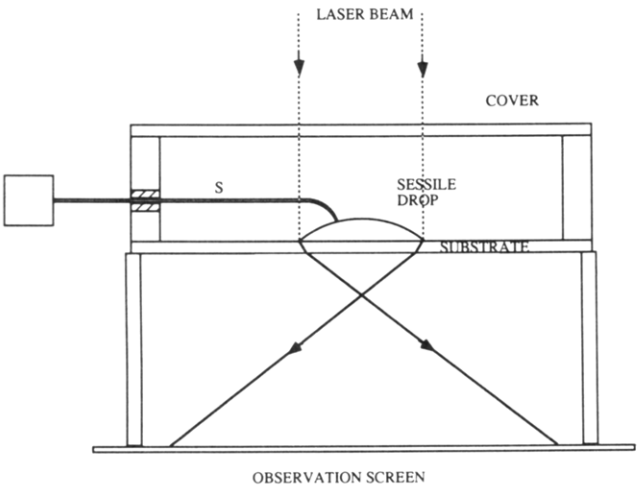

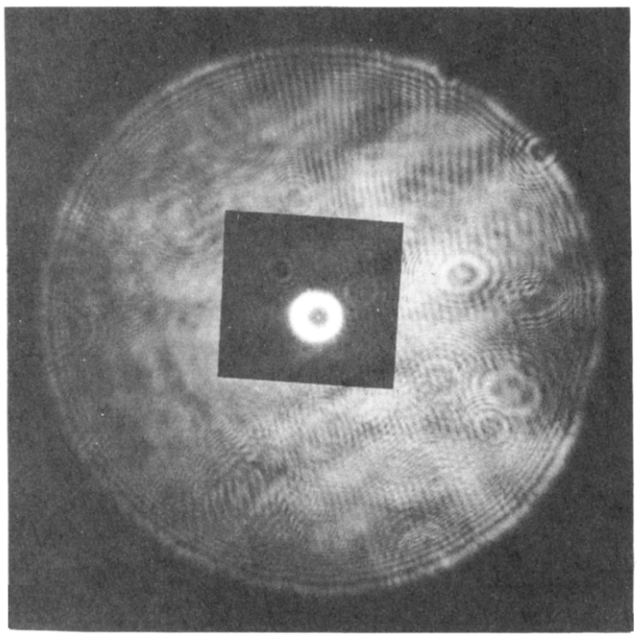

Figure 1. (a, Top) experimental apparatus. (b, Bottom) transmission pattern observed on the screen for a polymer droplet of diameter 3 mm deposited on an optically transparent slide. From the diameter D of the intercepted light cone, one deduces that the contact angle of the sessile droplet is 35° for this particular case. The bright circle in the center is the drop shadow. The larger central square is a piece of polarizer used to adjust the light intensity. The illumination is produced by a collimated polarized He–Ne laser.

the solutions were deposited with a wide-bore pipet (o.d. = 1 mm) and it was necessary to open the box for a few seconds. The contact angle was then measured as a function of time. Typical contact angle time variation is shown in Figure 2: it started from an initial value of 60° and reached a steady-state value of 45° after about 20 min for most of the viscous samples. In these cases, the relative accuracy on the advancing contact angle was again about 1%.

(2) Samples. Poly(styrene) solutions in toluene (purissimum grade) were prepared by weighing different amounts of polymer on a Mettler balance with 1-mg precision and then adding known volumes of solvent. The solutions were always prepared at the very last moment to minimize evaporation. The solutions were then continuously and gently agitated in sealed bottles for at least 1 week, up to the measurement time, to ensure complete homogenization. We checked the absence of solvent evaporation by controlling the solution weight just before use. Accuracy on ϕ was then about 1%. Several poly(styrene) samples were purchased from Toyo Soda (Tokyo). Their molecular weights and polydispersities are listed in Table I. The surface tension of pure toluene was taken from the literature to be 28.54 ± 0.05 mN·m^{-1}, at 20 °C.[15]

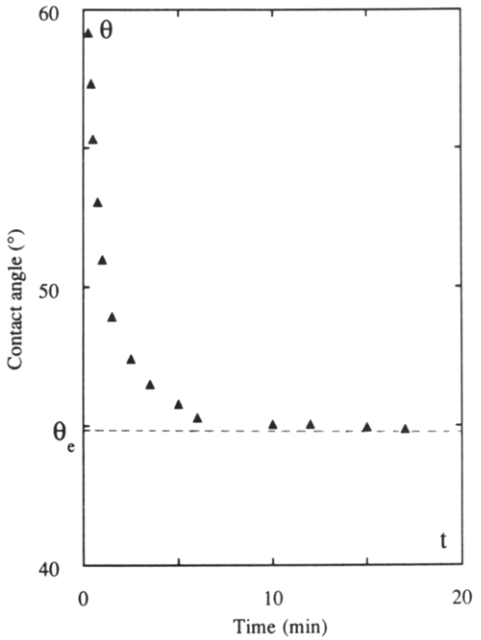

Figure 2. Typical time evolution of the contact angle after deposition of a polymer droplet from a wide-bore syringe, for a very viscous polymer solution (c = 0.18 g/g; M_w = 7.75 × 10^5).

Table I
Characteristics of the Polystyrene Samples

polymer sample	mol wt	polydispersity: M_w/M_n
1	107 000	1.01
2	422 000	1.05
3	775 000	1.01
4	2 890 000	1.09

(3) Solid Substrates. Fused silica slides (76 × 26 mm) of thickness 1.5 mm were used as the solid transparent substrates. They have a high-energy surface in their bare, clean, state. In order to ensure a repulsive situation for the solutions, they were chemically transformed into low-energy surfaces by grafting a monolayer of octadecyltrichlorosilane onto the surface hydroxyl groups according to the procedure of Sagiv, based on the deposition from solution method invented by Zisman.[16]

Results and Discussion

We have measured the advancing contact angle of sessile droplets on hydrophobic surfaces over a wide range of polymer concentration both in the dilute and semidilute (up to c = 0.35 g/g) regimes and for several molecular weights in the range 10^5–3 × 10^6.

(1) Dilute Regime. Following eq 11, we have plotted in Figure 3 the variation of $\Delta\theta$ with the polymer concentration c for one particular polymer molecular weight, M_w = 4.2 × 10^5. The contact angle values continuously increase from a value of θ = 34.44° for pure toluene up to a value of 41° for a polymer concentration of 0.1276 g/g. It is striking to observe that even a small amount of polymer chain is enough to modify the θ value. For instance, θ = 34.77° for c = 0.0062 g/g. All points fall on a straight line except for the last one which corresponds to a concentration of 0.1276 g/g. At this point, the solution is not in the dilute regime since, for this particular molecular weight, the crossover concentration to the semidilute regime is calculated to be c^* = 0.015 g/g.[17] In the dilute regime, the observed linear relationship between the contact angle increment and the polymer concentration is in good agreement with eq 11. Furthermore, the measured contact angle values are close enough to θ_0 to justify the approximation of replacing cos θ by cos θ_0 in the right-hand denominator of eq 6. This induces a systematic error which

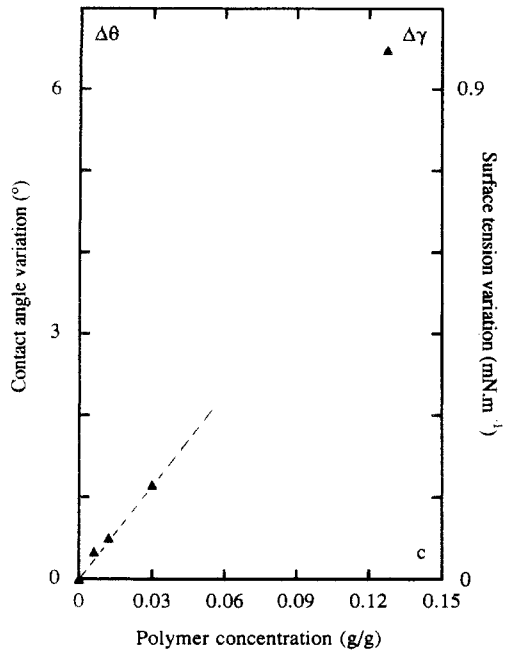

Figure 3. Variation of the contact angle, $\Delta\theta$, and of the surface tension, $\Delta\gamma$, with the polymer concentration, c. The poly(styrene) polymer has a molecular weight of 4.2×10^5. In the dilute regime ($c \ll c^*$), the contact angle increases linearly with the polymer concentration. The extreme right point on the curve exceeds the crossover concentration for polymer coil overlap ($c^* \approx 0.015$ g/g) and therefore no longer belongs to the dilute regime.

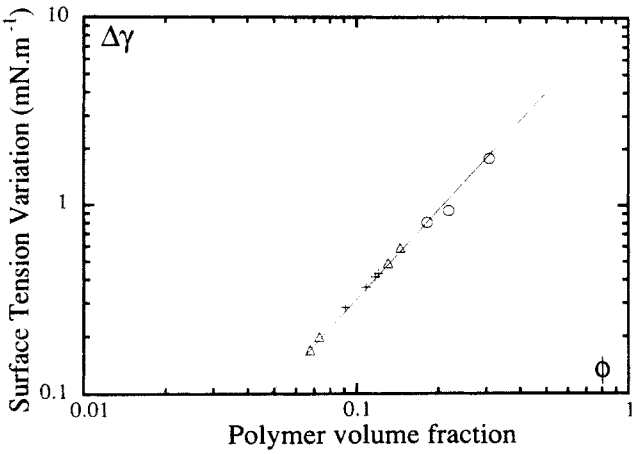

Figure 4. Dependence of the surface tension increment $\Delta\gamma$ with the polymer volume fraction ϕ. The various symbols corresponds to samples with different polymer molecular weights, M_w: 107 000 (×); 422 000 (○); 775 000 (+); 2 890 000 (△).

is always less than 3%. We have not attempted at this stage to test the dependence of θ on molecular weight. On the right-hand side of Figure 3, we have indicated the corresponding surface tension variations using the linear relationship predicted by eq 10. The slope of the dashed line corresponds to a surface tension increment of 6.2 $mN \cdot m^{-1}$ per g/g of polymer concentration.

(2) Semidilute Regime. The semidilute regime is illustrated in Figure 4 which is a log–log plot of the $\Delta\gamma$ variations with the polymer volume fraction ϕ. As explained in the theoretical section, this change of representation compared to the dilute regime is motivated by the fact that it is no longer possible in the semidilute regime to assume that $\Delta\theta$ is proportional to $\Delta\gamma$ and that ϕ is proportional to c. Therefore, the surface tension variation has been recalculated from the contact angle measurements using eq 6. The data points have been taken over volume fraction ϕ ranging from 0.06 to 0.3 and for four different molecular weights. The concentrations of first overlap, ϕ^*, are 0.06, 0.02, 0.01, and 0.004, respectively, and this sets the lower bound of ϕ for each molecular weight in order to study in the semidilute regime. We observe that all data points merge on a single curve which is actually a straight line with a slope 1.52 ± 0.05. This is fully consistent with the scaling predictions, $\Delta\gamma \sim \phi^{3/2}N^0$.

(3) Discussion. A simple consequence of our results is that measuring the contact angle of a sessile drop of a polymer solution provides a very simple means to know if one is dealing with a repulsive or with an adsorption case at the S/L and the L/V interfaces. For a repulsive case, the contact angle is expected to increase with the polymer concentration whereas, for the adsorption case, it should decrease with c. The method is extremely sensitive and the present data show a significant contact angle variation even for extremely low polymer concentrations. This has the advantage of limiting the amount of polymer required to perform the tests, which is particularly convenient when scarce materials or narrow molecular weight fractions have to be investigated. Moreover, the method is considerably cheaper to use than sophisticated methods such as neutron scattering or evanescent wave optical spectroscopy. It can also be performed on solid substrates with small areas (approximately a few square millimeters) which are easier to obtain, to control, and to clean.

In the particular case where both the S/L and the L/V interfaces are repulsive, it is possible to derive the surface tension dependence on solute concentration from the contact angle variation. Indeed, since the entropic interaction is of a very general nature and only involves the physical constraint that monomers cannot cross the interfaces, both interfaces behave identically. This is why we have written $\Delta\gamma_{ls} \approx \Delta\gamma_{lv}$. This assumption is fully justified by the excellent fit of experimental data to theory. The important consequence is that the general contact angle equation (4) then involves a single unknown, namely the liquid/vapor interfacial tension variation, $\Delta\gamma_{lv}$. This quantity can be derived univocally once one has measured the contact angle variation.

Dealing with the case where both interfaces are adsorbing would be more complicated. The surface tension variations are different at the liquid/solid and at the liquid/vapor interfaces since they depend on the strength of the polymer interactions with the adsorbing substrates, which have no reason to be identical at both interfaces. Moreover, a solid substrate may have specific adsorption sites for the polymeric chains. Measuring the contact angle is therefore not sufficient to derive the surface tension variations $\Delta\gamma_{ls}$ and $\Delta\gamma_{lv}$. Equation 4 now contains two unknowns, namely the liquid/vapor and the solid/liquid surface tensions. An independent determination of the surface tension variation at one of the walls by a second experimental method is therefore necessary to yield unambiguous results. On the other hand, it is still reasonable to assume that γ_{sv} is a constant because polymer chains are not volatile.

In the mixed case where one of the interfaces is repulsive and the other is adsorbing, the surface tension variations are evidently different at the L/S and at the L/V interfaces and one is returned to the last previous situation: equation 4 contains two unknowns, and the contact angle measurements cannot be related univocally to the surface tension variations. Our experimental observation that $\Delta\gamma$ scales as $\phi^{3/2}$, in the purely repulsive case, independent of molecular weight, and for concentrations higher than the overlap concentration c^*, is an important finding. First, the exponent value of the concentration dependence is

right on track with the theoretical value of $^3/_2$ predicted by the scaling argument for flexible chains in good solvent conditions. This result can be compared with an earlier determination by Ober et al.[15] of the liquid/vapor surface tension in the same polymer–solvent system. By using the de Nŏuy ring method, they were able to measure directly the surface pressure at the liquid/vapor interface. Their published value was 1.3 with a large error bar of 0.25. Since they were dealing with only two PDMS samples of nearly identical molecular weights, they had to study a large concentration range in order to extract a meaningful exponent. In the lower concentration limit ($c \approx c^*$), the relative accuracy for the surface tension measurement is poor. On the other hand, the upper concentration limit, in order to stay in the semidilute regime where the scaling theories apply, is not well-defined and one cannot be sure if the concentrated range has not been entered at the highest concentrations used in the experiments ($c \sim 0.35$ g/g for $M_w = 3 \times 10^5$). Depending on the cutoff for this upper concentration range, the exponent was found to be larger, up to 1.7. That can explain the rather large error bar on the exponent. By contrast, in our case, each of the solution concentrations has been taken in a narrow range above c^* in order not to exceed the semidilute regime, and we have used the molecular weight independence of the surface tension in the semidilute regime to obtain an overall wide concentration range. In addition, this is the first time that $\Delta\gamma$ is proved to be independent of molecular weight, which is a key point of the scaling theory. Translated in terms of the characteristic length, ξ, it means that, in the semidilute regime, ξ is independent of molecular weight. From the power law dependence of $\Delta\gamma$, one also obtains the dependence of ξ on polymer volume fraction ϕ: $\xi \sim \phi^{-3/4}$, independent of molecular weight, a result which has been established by EWIF[18] and neutron scattering[19] in good solvent conditions.

Finally, the contact angle method can be applied to various thermodynamic conditions of the polymer coils in solution. In the present paper, we have studied the good-solvent conditions and found an exponent of $^3/_2$ for the surface tension variation dependence on concentration. For theta solvent, one expects $\Delta\gamma \sim \phi^2$ which corresponds to $\xi \sim \phi^{-1}$. It therefore appears that the $\Delta\gamma$ dependence on ϕ is very sensitive to the thermodynamic quality of the solvent. Such experiments are currently under way in our laboratory.

Acknowledgment. We thank P. Pincus and F. Brochard-Wyart for their critical reading of the manuscript.

References and Notes

(1) Scheutjens, J. M. H. M.; Fleer, G. J. *J. Phys. Chem.* **1979**, *83*, 1619.
(2) Scheutjens, J. M. H. M.; Fleer, G. J. *J. Phys. Chem.* **1980**, *84*, 178.
(3) Scheutjens, J. M. H. M. Ph.D. Thesis, Lab. Phys. Col. Chem., Wageningen, The Netherlands.
(4) Joanny, J. F.; Leibler, L.; de Gennes, P. G. *J. Polym. Sci., Polym. Phys. Ed.* **1979**, *17*, 1073.
(5) de Gennes, P. G. *Scaling concepts in Polymer Physics*; Cornell University Press: Ithaca, NY, 1979.
(6) de Gennes, P. G. *Macromolecules* **1981**, *14*, 1637.
(7) Rondelez, F.; Ausserré, D.; Hervet, H. *Ann. Rev. Phys. Chem.* **1987**, *38*, 317.
(8) Barton, S. W.; Bosio, L.; Cortes, R.; Rondelez, F. *Europhys. Lett.* **1992**, *17*, 401.
(9) Lee, L. T.; Guiselin, O.; Lapp, A.; Farnoux, B.; Penfold, J. *Phys. Rev. Lett.* **1991**, *20*, 2838.
(10) Lee, L. T.; Guiselin, O.; Farnoux, B.; Lapp, A. *Macromolecules* **1991**, *24*, 2518.
(11) Guiselin, O.; Lee, L. T.; Farnoux, B.; Lapp, A. *J. Chem. Phys.* **1991**, *95*, 4632.
(12) *Polymer handbook*, 2nd ed.; Brandrup, J., Immergut, E. H., Eds.; John Wiley and Sons: New York, 1974; p 131.
(13) Allain, C.; Ausserré D.; Rondelez, F. *J. Colloid Interface Sci.* **1985**, *107*, 5.
(14) See ref 12, p 288.
(15) Ober, R.; Paz, L.; Taupin, C.; Pincus, P.; Boileau, S. *Macromolecules* **1983**, *16*, 50.
(16) Sagiv, J. *J. Am. Chem. Soc.* **1980**, *102*, 92.
(17) di Méglio, J. M.; Ober, R.; Paz, L.; Taupin, C.; Pincus, P. *J. Phys.* **1983**, *44*, 1035.
(18) Ausserré, D.; Hervet, H.; Rondelez, F. *Macromolecules* **1986**, *19*, 85.
(19) Auvray, L.; Cotton, J. P. *Macromolecules* **1987**, *20*, 647.

Registry No. PS, 9003-53-6.